Physics of the Earth and Planetary Interiors 301 (2020) 106453

Contents lists available at ScienceDirect

Physics of the Earth and Planetary Interiors

journal homepage: www.elsevier.com/locate/pepi

A study on the variations of recent seismicity in and around the Central Anatolian region of Turkey

S. Öztürk

Gümüşhane University, Department of Geophysics, TR-29100 Gümüşhane, Turkey

ARTICLE INFO

Keywords:
Central Anatolian region
b-value
Annual probability
Return period
GENAS modelling
Z-value

ABSTRACT

Variations of the recent seismicity in and around the Central Anatolian region of Turkey were evaluated based on the seismic *b*-value, standard normal deviate *Z*-value, *GENAS* modelling, annual probabilities and return periods of the earthquakes. The catalog includes 16,702 earthquakes between 1974 and 2019 with magnitudes from 1.0 to 6.3. Time distribution of *b*-value shows that there is a tendency to decrease after the year of 2002 and *b*-value decreased from 1.58 ± 0.03 to 1.25 ± 0.05 at the beginning of 2019. Annual probabilities for magnitude ranges of 3.0–4.0 have the values between 3 and 30. Return periods for magnitude levels of 5.0–5.5 have the values from 5 to 20 years, and a value of 80 years for magnitude level of 6.0. The *GENAS* results show the significant temporal variations in the number of earthquakes smaller and larger than specific magnitude intervals by supplying the beginning periods of increases and decreases in the earthquake activity rate. Remarkable reductions in region-time distribution of *b*-value at the beginning of 2019 were detected in the regions covering Niğde fault and its vicinity along the south, west, northwest and southwest directions, among the Mut Fault Zone, Karsantı-Karaisalı Fault Zone and Karataş-Osmaniye Fault Zone, in and around Sürgü fault and along its northwest direction, between Sürgü fault and East Anatolian Fault Zone. Significant seismic quiescence areas in *Z*-value distribution include the northwest ends of the Tuzgölü Fault Zone and study area including Akpınar fault, the northeast of Salanda fault, between Salanda fault and the Central Anatolian Fault Zone, the northeast parts of the Central Anatolian Fault Zone, the west of Malatya fault, between Sürgü fault and the East Anatolian Fault Zone, the southeast end of the Tuzgölü Fault Zone, Karsantı-Karaisalı Fault Zone and its vicinity, the southwest of Tuzgölü. Thus, these anomaly areas observed in the Central Anatolian region and its vicinity at the beginning of 2019 may be one of the most likely zones for the next strong/large earthquake occurrences.

1. Introduction

Identification of the region-time characteristics of earthquake occurrences can be achieved by many different statistical methods. There are quite effective approaches in the literature to understand the regional and temporal changes of seismic and tectonic activities. For a more quantitative assessment of seismic properties in a given region, several basic and the most frequently used scaling parameters such as seismotectonic *b*-value, seismic quiescence *Z*-value, *GENAS* modelling, annual probabilities and return periods of the earthquake occurrences can be preferred to provide preliminary helpful findings.

The frequency of earthquake occurrence and magnitude has been defined empirical magnitude-frequency relation and known as the *b*-value of Gutenberg-Richter relation (Gutenberg and Richter, 1944). This power law distribution is the most famous relationship in the statistical seismology and seismic hazard studies because it is necessary to estimate the return periods of the strong/large earthquakes. Regional and temporal changes of *b*-value can be used to define the properties of the seismic and tectonic environments, region-time-depth changes of stress and relative proportion of the small and great earthquakes (Scholz, 1968). Generally speaking, if there is a decreasing trend in *b*-value for a given region, it can be interpreted that there is a probability of earthquake occurrences. Another important tool for the description of region-time behaviors of the seismicity can be given as the assessment of the seismicity rate changes. Wyss and Martirosyan (1998) defined the precursory seismic quiescence (*Z*-value) as a significant decrease in the mean seismicity rate in comparison with the background activity rate. This quiescence period can be observed in focus areas and its vicinity in several years before main shock time, or this decrease may be separated from the main shock by a relatively short period with a tendency to increase in seismicity (Wyss and Habermann, 1988). Analysis of the seismicity rate changes is an important step to estimate

E-mail address: serkanozturk@gumushane.edu.tr.

https://doi.org/10.1016/j.pepi.2020.106453
Received 24 July 2019; Received in revised form 23 February 2020; Accepted 23 February 2020
Available online 24 February 2020

the seismic hazard because the quiescence period depends strongly on seismic and tectonic environments. In addition to *b* and *Z*-values, The *GENAS* algorithm has been used to evaluate the important changes in different magnitude groups. The *GENAS* technique (Habermann, 1983) describes important changes in earthquake activity rate and provide the time-number distribution of earthquakes bigger and lower than a specific magnitude level (Chouliaras, 2009). Thus, the *GENAS* test is a significant tool in the assessing of all significant seismic activity rate changes with respect to time.

The main purpose of this investigation is to supply preliminary insights for a reliable evaluation of region-time seismicity patterns of the Central Anatolian region of Turkey and its vicinity. These types of techniques have been applied in many statistical studies in different regions worldwide and also Turkey, and some important results have been obtained in recent years (e.g., Frohlich and Davis, 1993; Console et al., 2000; Wu and Chiao, 2006; Polat et al., 2008; Katsumata, 2011; Öztürk, 2013, 2017, 2018; Gök and Polat, 2014; Rehman et al., 2015; Negi and Paul, 2015; Ali, 2016; Raub et al., 2017; Ormeni et al., 2017; Ozer et al., 2018, 2019; Rodriguez-Perez and Zuniga, 2018; Chiba, 2019; Coban and Sayil, 2019; Uner et al., 2019).

2. Seismotectonic properties of the Central Anatolian region and its vicinity

Turkey is one of the most seismically and tectonically active zones in the world. Tectonic mobility in Turkey and its vicinity arises from the relative motions between surrounding plates such as the Aegean, African, Arabian, Anatolian, Black Sea and Eurasian plates. Turkey is located in the Mediterranean part of Alpine-Himalayan orogenic system and the most important tectonic environments can be stated as the Caucasus, Aegean Arc, West Anatolian Graben Systems (WAGS), North Anatolian Fault Zone (NAFZ), East Anatolian Fault Zone (EAFZ), North East Anatolian Fault Zone (NEAFZ), Bitlis-Zagros Thrust Zone (BZTZ) and Dead Sea Fault Zone (DSFZ).

It is well known that the Central Anatolian region (CAR) of Turkey has not an important seismic hazard with regard to occurrences of the large or destructive earthquakes in the short and intermediate terms. However, several strong/large events occurred in the CAR and its surrounding regions in the past and recent years such as; July 4, 1978 Bala-Ankara (*M*5.3), December 28, 1979 Kozan-Adana (*M*5.3), April 21, 1983 Bala-Ankara (*M*5.0), June 27, 1998 Hasanbeyli-Adana (*M*6.3), June 25, 2001 Arslanlı-Osmaniye (*M*5.5), December 14, 2002 Andırın-Kahramanmaraş (*M*5.6), December 20, 2007 Bala-Ankara (*M*5.7), December 27, 2007 Bala-Ankara (*M*5.5), February 16, 2012 Malatya-Darende (*M*5.0) and January 10, 2016 Hacıduraklı-Kırşehir (*M*5.1). Thus, because of the occurrence of recent strong/large earthquakes, seismic hazard studies for this region have become more important. Details of earthquake occurrences in and around the CAR were also provided in Table 1.

The Central Anatolian region is one of the most important tectonic regions in Anatolia, Turkey. The eastern pressure and the western extension regimes are quite effective on this placement. NS and NNE-SSW shortening are dominant in the CAR and its vicinity, and the collisional motions between Anatolian and African plates along the Cyprian have a great influence on this shortening (Bozkurt, 2001). Fundamental tectonic structures in and around the CAR can be given as Tuzgölü Fault Zone (TGFZ), Central Anatolian Fault Zone (CAFZ), Karsantı-Karaisalı Fault Zone (KKFZ), Akpınar fault (AF), Niğde fault (NF) and Salanda fault (SF). In addition, study area is covered by the NAFZ, Yağmurlu-Ezinepazarı Fault Zone (YEFZ) and Taşova-Çorum Fault Zone (TÇFZ) in the north, Beyşehir Graben (BG), Akşehir Fault Zone (AFZ) and Akşehir-Afyon Graben (AAG) in the west, Yakapınar-Göksun Fault Zone (YGFZ), Karataş-Osmaniye Fault Zone (KOFZ), EAFZ, Bozova fault (BZF) and DSFZ in the southeast, Mut Fault Zone (MFZ) in the southwest, Sürgü fault (SRF), Malatya fault (MF) and Ovacık fault (OF) in the east. These fault systems both in the extensional and compressional study area has characterized by oblique-slip faults, mostly dextral and sinistral strike-slip faults. Details on seismic and tectonic structures for this region can be found in different sources as Bozkurt (2001), Özsayın and Dirik (2007), and Gökten and Varol (2010). Fundamental tectonic structures in the CAR and surroundings were drawn from different sources such as Şaroğlu et al. (1992), Bozkurt (2001), Ulusay et al. (2004) and plotted Fig. 1a.

3. Earthquake catalog and definition of the methods for the statistical analyses

Data catalog used in this statistical study was compiled from Öztürk (2009) during the time periods of 1970–2006. The catalogs from Bogazici University, Kandilli Observatory and Research Institute (KOERI) and Disaster and Emergency Management Authority (AFAD) were also combined for the time interval between 2006 and 2019. For the statistical region-time assessing, an original database including 16,702 shallow (depth < 70 km) earthquakes from September 1974 to December 2018 with magnitude range between 1.0 and 6.3 was used. Earthquake catalog is homogenous with respect to duration magnitude, M_d, and time length of the catalog is nearly 44.29 years. Epicenter distributions of all 16,702 events were shown in Fig. 1b by using different symbols for different magnitude groups.

Separation of dependent earthquakes from the catalogs is a significant stage for reliable and high quality seismic hazard analyses. For this reason, earthquake catalogs need to be declustered and earthquakes must be separated into main and secondary events. At the end of this process, all dependent earthquakes are separated from independent ones and these dependent events are substituted with a unique event by eliminating each cluster. In this study, declustering method based on the algorithm modeled by Reasenberg (1985) method was preferred in order to decluster the earthquake catalog through *ZMAP* software (Wiemer, 2001). This declustering algorithm presents some artificial manipulations. In fact, declustering process includes some arbitrary input parameters such as the look-ahead time for un-clustered events, the maximum look-ahead time for clustered events, the effective lower magnitude cutoff for the catalog, the factor for the interaction radius of dependent events, etc. These parameters allow to researchers to remove all the dependent events in a smaller/larger time or space interval according to the main shock epicenter (one can find many details for these parameters in Reasenberg, 1985). Since this method has been widely applied for different earthquake catalogs, all the input parameters for the earthquake declustering in this study were accepted as the same in Reasenberg (1985). Also, magnitude completeness, *Mcomp*, is a very significant parameter for the statistical seismicity studies. *Mcomp* is the minimum magnitude of complete recording and can be calculated from magnitude-frequency distribution of earthquakes (Wiemer and Wyss, 2000). This magnitude level contains the 90% of the earthquakes in the catalog and temporal changes in *Mcomp* can affect the results of the seismicity parameters, especially in *b* and *Z*-values. Therefore, the maximum number of earthquakes in the catalog was aimed to be used for high-quality results for the analysis of all statistical parameters. In this study, all statistical region-time analyses were performed with *ZMAP* software package introduced by Wiemer (2001).

After declustering process, 1595 earthquakes (approximately 9.55%) were eliminated and 15,107 earthquakes left. For the original catalog including all shallow earthquakes with $M_d \geq 1.0$, *Mcomp* changes between 1.7 and 3.6 from 1974 to 2019 and hence, it was used as 2.6 on average (Fig. 2). Since magnitude completeness analysis is quite effective on the correct estimation of *b*-value, *Z*-value, annual probability, return period and the *GENAS* modelling, temporal *Mcomp* was analyzed and estimated with great care. The number of earthquakes with magnitude $M_d < 2.6$ are 8633 and all earthquakes with magnitude $M_d < 2.6$ were separated from the catalog. Finally, after declustering and separating $M_d < 2.6$ earthquakes, nearly 61.24% of all events was removed and the number of earthquakes for seismic

Table 1
Details of the strong/large earthquakes occurred in and around the Central Anatolian region of Turkey.

Year	Month	Day	Origin time	Latitude	Longitude	Depth (km)	Magnitude (M_d)	Environment
1978	07	04	22:39:16	39.45	33.19	23.0	5.3	Ankara
1979	12	28	03:09:08	37.52	35.85	47.0	5.3	Adana
1983	04	21	16:18:57	39.31	33.06	36.0	5.0	Ankara
1989	06	24	03:09:58	36.71	35.93	46.0	5.1	Antakya
1994	01	03	21:00:30	37.00	35.84	26.0	5.0	Adana
1998	06	27	13:05:51	36.96	35.52	18.0	6.3	Adana
1998	07	04	02:15:47	36.85	35.47	35.0	5.1	Adana
2001	06	25	13:28:48	37.12	36.28	27.0	5.5	Osmaniye
2001	10	31	12:33:52	37.17	36.22	11.0	5.2	Osmaniye
2002	12	14	01:02:43	37.47	36.31	7.0	5.6	Kahramanmaraş
2007	12	20	11:48:27	39.40	33.05	5.0	5.7	Ankara
2007	12	27	01:47:08	39.42	33.09	5.0	5.5	Ankara
2010	02	01	06:01:40	39.58	38.01	5.0	5.0	Sivas
2012	02	16	13:01:03	38.65	37.46	3.1	5.1	Malatya
2015	07	30	01:00:54	36.51	35.07	21.5	5.2	Adana
2016	01	10	19:40:47	39.58	34.36	5.0	5.1	Kırşehir

hazard analysis was reduced to 6474 (Fig. 3). Thus, this more robust, homogeneous and reliable earthquake catalog was used as the final data catalog.

3.1. Gutenberg-Richter relation (magnitude-frequency distribution, b-value), annual probability and return period

Gutenberg and Richter (1944) size-scaling relation is known the basic form of earthquake statistics in seismology. This empirical power-law relation describes the magnitude-frequency distribution of earthquake occurrences and the mathematical formula of this form is defined by:

$$\log_{10} N(M) = a - bM \tag{1}$$

where *N(M)* is the cumulative number of earthquakes in a particular time period with magnitudes equal to or larger than *M*, while *a* and *b*-values are constants. Changes in *a*-value are related to the size of the study region, duration of the catalog and also earthquake numbers. Therefore, *a*-value exhibits significant changes for different regions in relation to the earthquake activity level. *b*-value can be calculated from the slope of magnitude-frequency curve. It is one of the most principal applications in earthquake physics and plays a significant role in the description of realistic design earthquakes for a given region. It is suggested that variations in *b*-value are generally between 0.3 and 2.0 for different seismic zones worldwide (Utsu, 1971). In addition, Frohlich and Davis (1993) defined the average *b*-value as close to 1.0. Although *b*-value reflects the relative numbers of small and great earthquakes, it is, in fact, a quite important parameter in terms of rheological and geotechnical perspective, and many factors affect the variations in *b*-value. According to the results of laboratory studies for rock fracture, a tendency to decrease is related to a reduction in the confining pressure and an increase in the applied shear stress (Scholz, 1968). However, large *b*-values are related to an increase in the thermal gradient, fracture density, or material heterogeneity in the geological complexity (Mogi, 1962). Previous studies show that *b*-value is also related to the material properties, fault length, strain circumstances and slip distribution etc., and it is scale invariant.

Annual probabilities of any earthquakes with different magnitude levels and within any period can be estimated from following mathematical formula (Ali, 2016):

$$P(M) = 1 - e^{-N(M)*T} \tag{2}$$

where *P(M)* is the probability that at least one event will occur in specific *T* years. *M* is taken from Eq. 1. Also, return periods of any earthquakes with different magnitude values can be estimated from following equation (Ali, 2016):

$$Q = 1/N(M) \tag{3}$$

3.2. Precursory seismic quiescence (Z-value) and GENAS modelling

The phenomenon of precursory seismic quiescence was firstly proposed by Wyss and Habermann (1988) and then Wiemer and Wyss (1994) introduced a methodology that can be performed in *ZMAP* software. Researchers have used different techniques to describe and characterize the seismicity rate changes for different parts of the world and most of them use region-time modelling of precursory quiescence before the main earthquakes. One of the most popular technique among them is well known as the standard normal deviate *Z*-test and many applications on *Z*-value can be found in literature. Therefore, a brief description of this technique will be provided in this section (for details, see Wiemer and Wyss, 1994).

ZMAP application provides a continuous image of seismicity rate changes and the regions exhibiting seismic quiescence in region and time can be plotted in geographical coordinates. *Z*-test is applied to detect the precursory quiescence regions and Long Term Average (LTA) function is generated for the statistical assessment of confidence level in standard deviation units:

$$Z(t) = \frac{R_{all} - R_{wl}}{\left(\frac{\sigma_{all}}{n_{all}} + \frac{\sigma^2_{wl}}{n_{wl}}\right)^{1/2}} \tag{4}$$

where R_{all} is the mean activity rate in the overall foreground period, R_{wl} is the average number of earthquakes in the background window, σ and n are the standard deviations and the number of samples within and outside the window, respectively. *Z*-value estimated as a function of time lets the foreground window slide along the time period of catalog and is called as LTA. The shape of LTA function depends on the selection of the time window (Tw). Statistical robustness of the LTA function increases with the size of Tw and its shape becomes more and more smooth if Tw exceeds the duration of the anomaly. Quiescence period is also a significant parameter to be estimated and its importance is maximized when Tw is equal to that value. However, the results do not depend on the selection of Tw. Since the quiescence period is not known, time window changes between 1.5 and 5.5 years because these lengths are in the range of reported seismic quiescence prior to the crustal main shocks (Wyss, 1997).

The *GENAS* algorithm defines major variations in seismic activity rate by considering the number of earthquakes smaller and larger than a specific magnitude level as a function of time (Habermann, 1983; Zúñiga et al., 2005; Chouliaras, 2009). This technique also allows to users to detect the times that stand out as the beginning of periods were increase and/or decreases earthquake activity are identified as well as

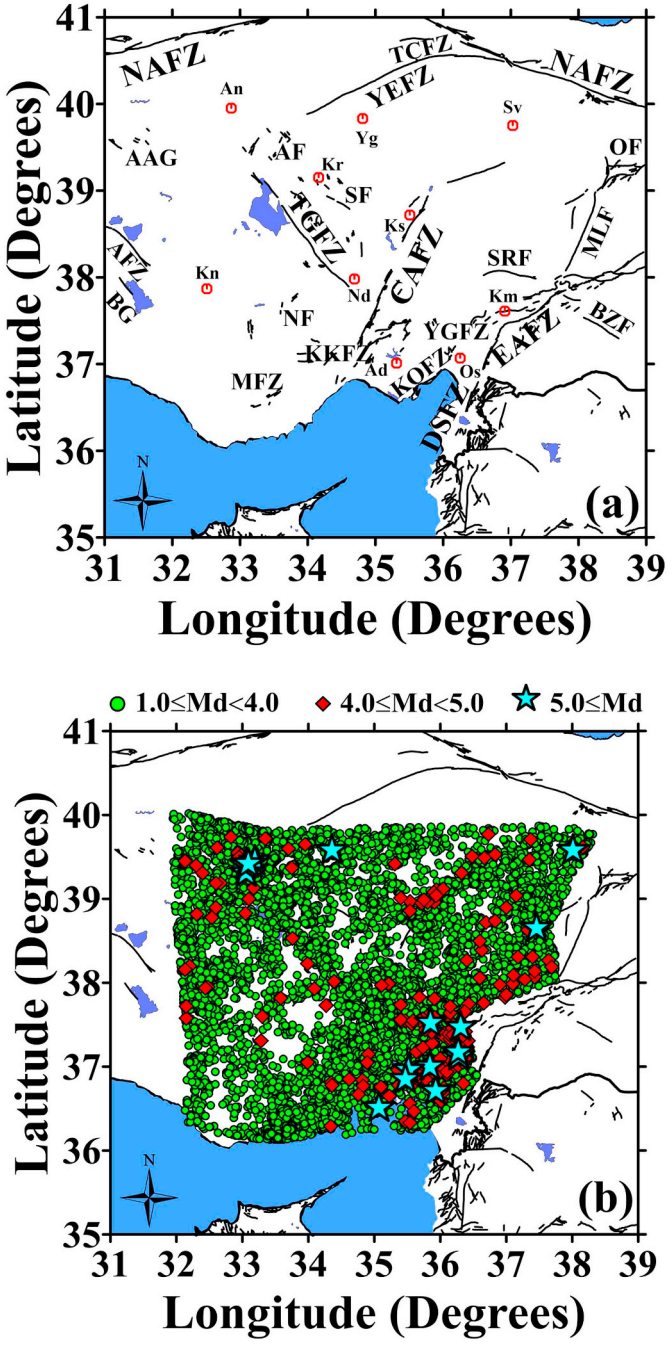

Fig. 1. (a) Simplified tectonic environments from Şaroğlu et al. (1992), Bozkurt (2001) and Ulusay et al. (2004). Names of the faults were given in the text and also some provinces in and around the study region were provided on the figure. An: Ankara, Yg: Yozgat, Sv: Sivas, Kr: Kırşehir, Ks: Kayseri, Kn: Konya, Nd: Niğde, Km: Kahramanmaraş, Os: Osmaniye, Ad: Adana. (b) Epicenter distributions of original dataset consisting of 16,702 shallow earthquakes with $M_d \geq 1.0$ from 1974 to 2019 for the CAR and its vicinity. Magnitude values of the events were symbolized with different indicators.

the magnitude range influenced by these variations (Zúñiga et al., 2000). The *GENAS* modelling estimates the cumulative number of earthquakes in specific magnitude levels and is based on the iterative comparison of the seismic activity rates in different magnitude ranges. The main goal of the considering the earthquake numbers of different magnitude levels separately is to evaluate understandably the individual variations in specific magnitude ranges. Thus, the *GENAS* algorithm provides a preliminary, general and useful overview for the earthquake history as well as to give periods and fluctuation intervals (Zúñiga et al., 2000, 2005; Chouliaras, 2009).

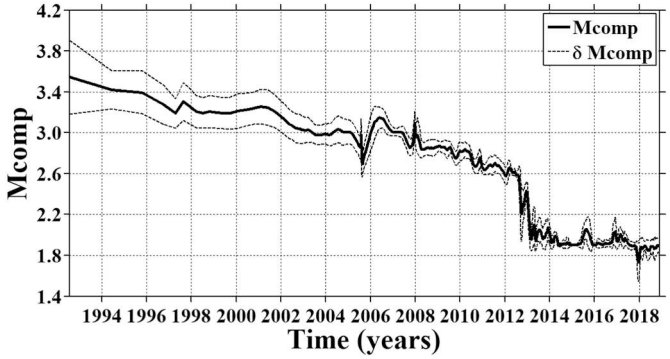

Fig. 2. Magnitude completeness, *Mcomp*, as a function of time. Standard deviation, *δMcomp*, was provided with dashed line. Completeness analysis was sampled with an overlapping techniques and each sample includes 250 earthquakes.

4. Results

In the present work, the principal aim is to obtain some preliminary results for seismic hazard and risk by providing a region-time analysis of seismotectonic parameters for the CAR of Turkey at the beginning of 2019. For this type of comprehensive statistical analysis, this work addressed the time-magnitude distribution of earthquake activity, magnitude completeness with time, changes of *b*-value and *Z*-value in regional and temporal scale, *GENAS* modelling, annual probabilities and return periods of the earthquakes, and their interrelationships. Consequently, recent and future seismic potential were tried to present by supplying useful evidences to the next earthquake occurrences in the real time for the CAR and its vicinity.

The estimation of magnitude completeness is very important for the selection of the minimum magnitude of complete recording in seismicity studies including statistical region-time analyses. Therefore, temporal variation of *Mcomp* and its standard deviation was plotted and given in Fig. 2. Estimation of *Mcomp* as a function of time was achieved by using a moving window technique. Original catalog including 16,702 earthquakes was used and sampled with 250 events per window for the estimation of *Mcomp*. It is relatively large and varies from 3.0 to 3.6 between 1974 and 2004 whereas it changes from about 3.0 to about 2.6 between 2004 and 2012. Then, *Mcomp* varies from 2.6 and 2.0 between 2012 and 2014 while it decreases to about 1.8 at the beginning of 2019. Thus, temporal *Mcomp* shows a non-stable change from 1.7 to 3.6 between 1974 and 2019 as shown in Fig. 2. From this temporal analysis for the estimation of *Mcomp*, an average *Mcomp* was assumed as 2.6 and this completeness value was used to estimate all the seismicity parameters.

Fig. 3 shows the cumulative number of events as a function of time for the original data set including all earthquakes with $M_d \geq 1.0$ (16,702 earthquakes), for the declustered data set with $M_d \geq 1.0$ (15,107 earthquakes) and for the declustered data set with $M_d \geq 2.6$ (6474 earthquakes). As shown in Fig. 3, there is not any significant earthquake activity from 1974 to 1995 and a little seismicity changes was observed between 1995 and 2000. However, an important increase in seismicity can be seen after 2000 and especially after 2005. Moreover, data set can be considered separately homogeneous between 1974 and 1995, 1995 and 2005, and between 2005 and 2019. Many observatories in Turkey have established seismic stations and especially two of them, KOERI and AFAD have provided real time data in and around the study region in recent years. Hence, the minimum level of recording magnitude shows a tendency to decrease up to 2.6. Several researchers achieved comprehensive spatial and temporal analyses on

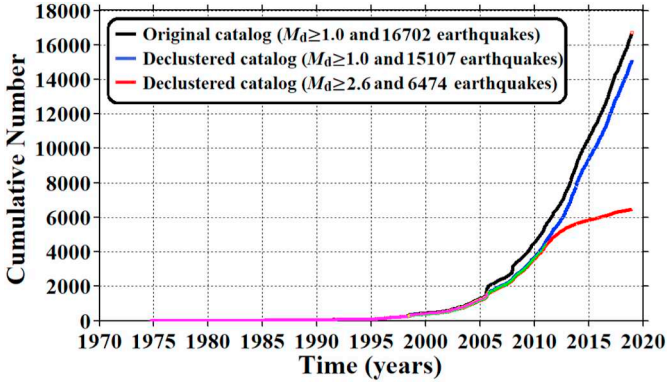

Fig. 3. Cumulative number plot of earthquakes as a function of time for the original data set including all earthquakes with $M_d \geq 1.0$, for the declustered data set with $M_d \geq 1.0$ and for the declustered data set with $M_d \geq 2.6$.

the statistical seismicity characteristics (e.g., Katsumata and Kasahara, 1999; Joseph et al., 2011). These authors stated that the selection of the magnitude completeness and declustering of the earthquake catalog are very significant stage for the statistical estimations of earthquake occurrences. These studies show that a completeness analysis must be done and all dependent earthquakes such as foreshocks, aftershocks and swarms must be removed from the catalog before starting any calculations. As shown in Fig. 3, the cumulative number of declustered events with $M_d \geq 2.6$ has a smoother slope than that of the original catalog. Thus, these two processes eliminated the dependent events from the original catalog. It is a remarkable fact, after the application of declustering process and completeness estimation, a more reliable, homogeneous and robust data set was supplied for the statistical region-time analyses.

Fig. 4 shows magnitude and time histograms of the earthquake occurrences in and around the CAR. As mentioned in Data section, earthquake magnitudes vary from 1.0 to 6.3 and the numbers of earthquakes have an exponential decay from smaller to larger sizes. As seen in Fig. 4a, magnitudes of the most earthquakes vary from 1.5 to 3.5 and there is a maximum for $M_d \geq 1.9$. Also, the number of earthquakes has a maximum in $M_d \geq 2.6$ level. The number of the events with $1.5 \leq M_d < 3.5$ are 15,175. However, there are 798 earthquakes for $1.0 \leq M_d < 1.5$, 12,588 earthquakes for $1.5 \leq M_d < 3.0$, 3100 earthquakes for $3.0 \leq M_d < 4.0$, 200 earthquakes for $4.0 \leq M_d < 5.0$, and 16 earthquakes for $5.0 \leq M_d$. As a result, earthquakes with a magnitude of 1.5–3.5 occur more frequently than those of the others in the CAR and its vicinity. This tendency to increase in the number of small earthquakes may be an indication of stress increase in the CAR in recent years. Time histogram of the earthquake occurrences between 1974 and 2019 was also plotted in Fig. 4b. The seismicity from 1974 to 2003 varies very little and the number of events for all magnitude sizes in this time period is 762. Although earthquake activity between 2003 and 2010 shows both strong increases and decreases, there is a general increase in the number of earthquakes after 2010. There are 3748 events between 2003 and 2010 whereas there are 12,192 earthquakes between 2010 and 2019. However, systematic increase in seismicity shows a decreasing trend between 2015 and 2016, and the total number of earthquakes between these years is 2836. Also, a maximum increase in the number of earthquakes was reported in 2016 as 1651 events. As a significant result, these types of statistical applications may give helpful preliminary results for the analysis of earthquake occurrence rate and these evaluations can be attributed with the region-time variations of precursory seismicity rate changes in and around the CAR.

Annual probabilities and return periods of different magnitude values were plotted in Fig. 5. As stated in Joseph et al. (2011), declustering process and magnitude completeness estimation should be realized for the statistical assessment of seismicity characteristics, especially in the return period estimation of earthquakes. Therefore, declustered dataset including *Mcomp* (6474 events) was preferred in these applications. Annual probabilities of the seismic activity in different magnitude levels indicate relatively larger values ranging from 1 to 30 for the earthquakes of $3.0 \leq M_d < 4.5$, and the values relatively

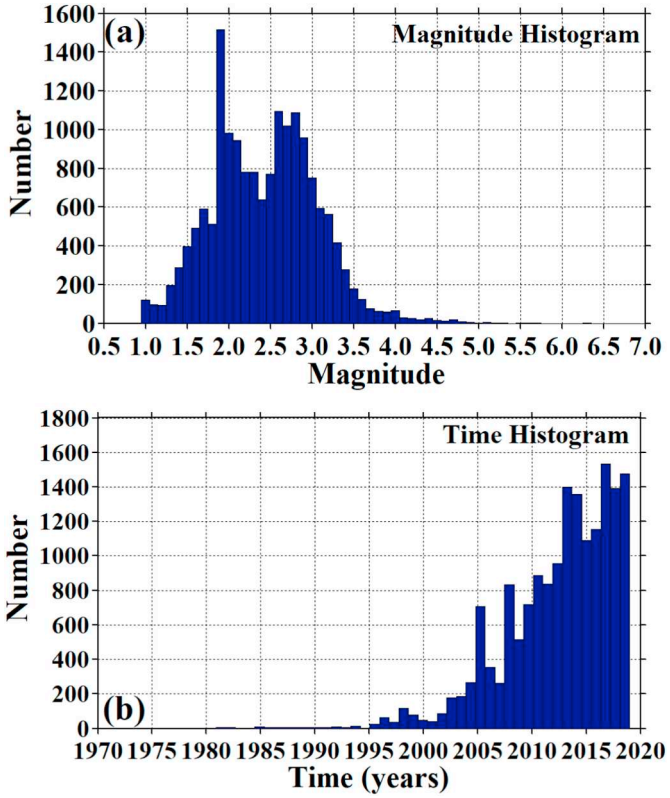

Fig. 4. (a) Magnitude histogram and (b) Time histogram of the seismicity in the CAR and vicinity from 1974 to 2019.

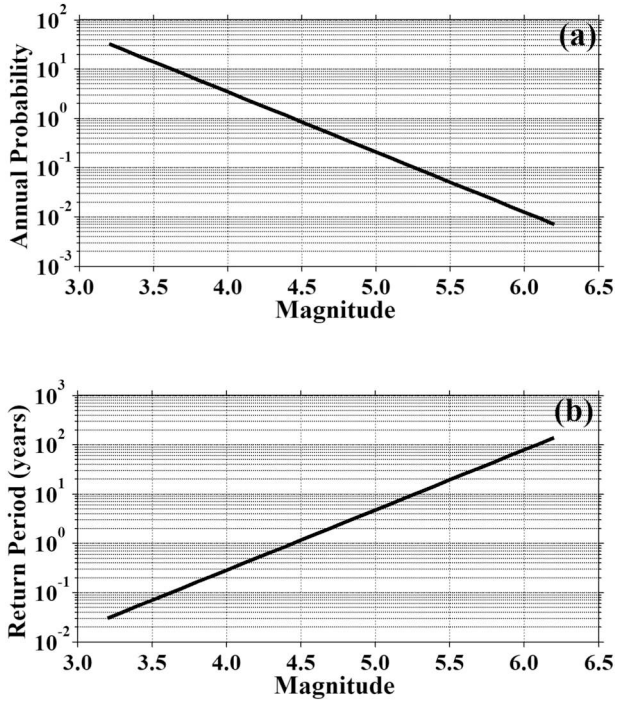

Fig. 5. (a) Annual probability and (b) Recurrence time of the earthquake occurrences as a variable of magnitude.

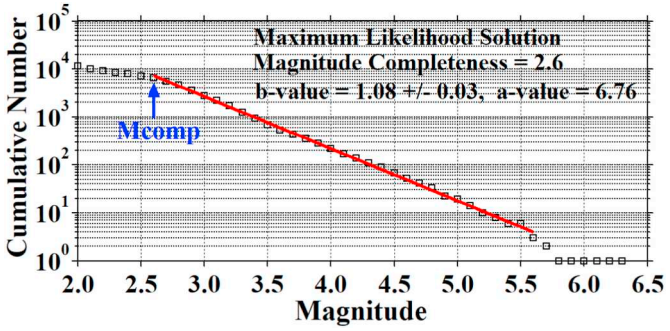

Fig. 6. *b*-value of the Gutenberg-Richter relationship and magnitude-frequency distribution. Declustered earthquake catalog including 15,107 earthquakes was used for the analysis and *Mcomp* was also marked on the figure.

smaller than 1 for the events of $4.5 \leq M_d$ (Fig. 5a). Return periods of the earthquake activity in different magnitude values were also represented in Fig. 5b. Return periods smaller than 1.0 year were calculated for the earthquakes of $3.0 \leq M_d < 4.5$. Intermediate return periods ranging from 1 to 10 years were estimated for the earthquakes of $4.5 \leq M_d < 5.3$, and return periods ranging from 10 to 20 years can be expected for the earthquakes of $5.3 \leq M_d \leq 5.5$. Also, return periods larger than 20 years (between 20 and 150 years) were calculated for the earthquakes of $5.5 < M_d$ (Fig. 5b). These results show that earthquake occurrences ranging from 3.0–4.5 magnitude level are more likely than those of the other occurrences, and a strong earthquake $5.0 < M_d$ can be occurred in every ten years. These results can also be supported from Table 1 and these types of analyses can provide remarkable results to describe the statistical behaviors of strong/large earthquake occurrences in the CAR and its vicinity.

b-value of the Gutenberg-Richter relationship and magnitude-frequency distribution for the declustered catalog including 15,107 earthquakes was given in Fig. 6. *b*-value was calculated with the maximum likelihood method because this application provides a more robust estimate than the least-square regression technique (Aki, 1965). As shown in Fig. 2, average *Mcomp* for all dataset was considered as 2.6 and average *b*-value between 1974 and 2019 was calculated as 1.08 ± 0.03. In addition to *b*-value, its standard deviation, *a*-value and *Mcomp* were provided on Fig. 6. As mentioned above, *b*-value changes from 0.3 to 2.0 on global scale depending on region, and tectonic earthquakes are represented with a *b*-value between 0.5 and 1.5 although average *b*-value is accepted close to 1.0 (Frohlich and Davis, 1993). Thus, *b*-value of the earthquake occurrences in and around the CAR is well represented by the Gutenberg-Richter power law distribution with the *b*-value close to 1.0.

Temporal changes of *b*-value were given in Fig. 7. In order to calculate the changes in *b*-value as a function of time, time duration of the catalog was divided into four different time intervals by considering the fluctuations in specific times in Fig. 7, and *b*-values for these time periods were plotted as in Fig. 8. For the calculation of temporal *b*-value variation, declustered earthquake catalog (15,107 earthquakes) was used and overlapping samples were considered as 150 events per window. As seen in Fig. 7, there are significant decreases and increases in certain years such as 2002, 2008 and 2013. Hence, specific time intervals were selected as 1974–2002, 2002–2008, 2008–2013 and 2013–2019 considering the temporal characteristics Fig. 7, and then *b*-values were estimated separately as shown in Fig. 8. Different earthquake numbers and *Mcomp* values were used for each time interval due to size variations of time period and earthquake density in each period. There are not any significant variations in *b*-value from 1974 to 2002 and average *b*-value was calculated as 0.98 ± 0.09 with *Mcomp* = 3.3 by using 534 earthquakes (Fig. 8a). There are great increases and decreases in *b*-value from 2002 to 2008 and average *b*-value was computed as 1.58 ± 0.03, a larger value compared to that of the previous time interval, with *Mcomp* = 3.0 by using 1887 events (Fig. 8b). There are great fluctuations and a systematic increase in *b*-value from 2008 to 2013, with a sharp decrease at the beginning of 2012, and average *b*-value was found as 1.48 ± 0.03, a smaller value than that of the previous period, with *Mcomp* = 2.6 by using 4098 earthquakes (Fig. 8c). However, for the last time period between 2013 and 2019, there is a clear decrease in *b*-value and average *b*-value was estimated as 1.25 ± 0.05, a lower value than that of the previous period, with *Mcomp* = 2.0 by using 8588 earthquakes (Fig. 8d). As shown in Fig. 7, there is a clear increase in *b*-value from 2002 to 2012, while there is a clear decrease after 2013. Moreover, significant fluctuations are related to the occurrence times of the strong/large earthquakes from 2000 to 2017 (also can be seen from Table 1). There are 16 strong/large earthquakes (see Fig. 1 and Table 1) and a clear decreasing trend can be seen in *b*-value before these main shocks. As mentioned above, many researchers such as Öztürk (2011, 2018) and Ormeni et al. (2017) detected these types of decreases before the occurrences of some great earthquakes. It is well known that there are many factors affecting *b*-value variations. From these results, one can conclude that decreasing trend in *b*-value before the main events may be resulted from increasing stress distribution and this decrease in *b*-value in recent years may be considered as a precursor of the next probable earthquakes in and around the CAR.

Temporal magnitude distribution of the earthquakes for $4.0 \leq M_d$ in and around the CAR was illustrated in Fig. 9. Magnitude variations of earthquakes with $4.0 \leq M_d$ were plotted in order to evaluate the changes in magnitude values from 1974 to 2019. As given in Table 2,

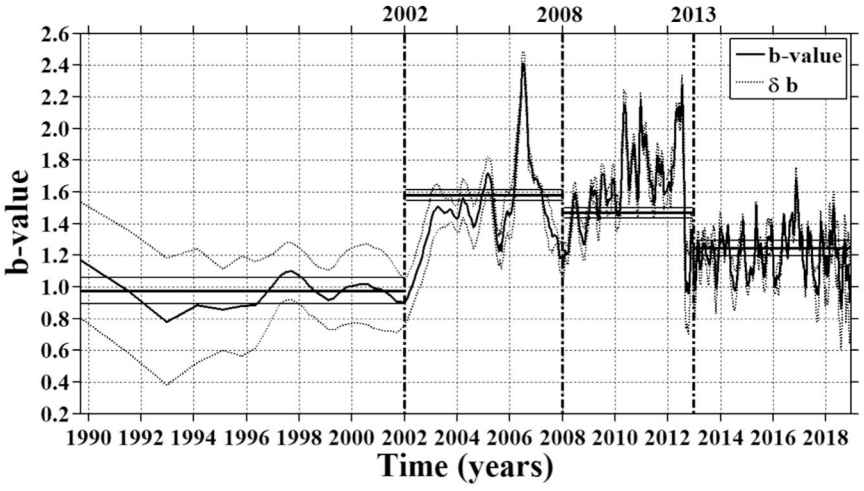

Fig. 7. *b*-value changes as a function of time and its standard deviation (dashed line, δ*b*). Thick horizontal lines indicate the mean *b*-values, and the upper and lower thin horizontal lines indicate their standard deviations. Declustered dataset was used for analysis and overlapping samples were considered as 150 earthquakes per window.

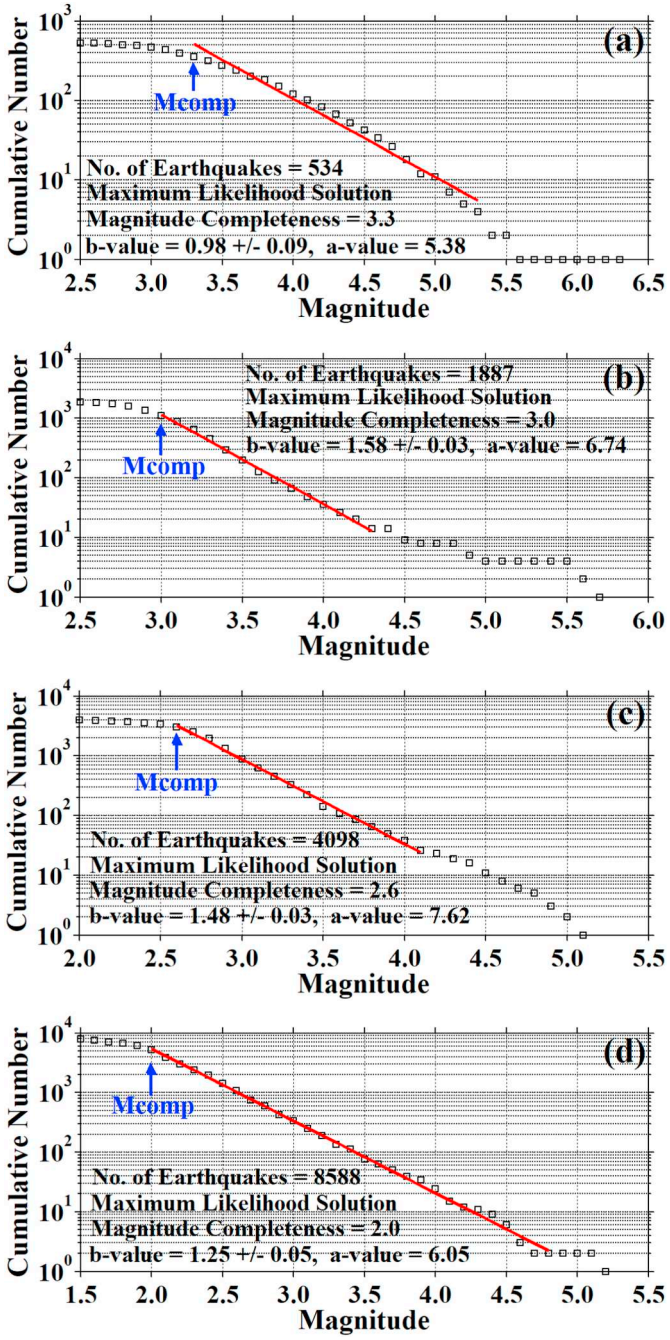

Fig. 8. *b*-value of the Gutenberg-Richter relationship and magnitude-frequency distribution of different time periods for (a) 1974–2002, (b) 2002–2008, (c) 2008–2013 and (d) 2013–2019.

average magnitude level is 4.38 ± 0.38 for the time period from 1974 to 2002, 4.38 ± 0.44 from 2002 to 2008, 4.38 ± 0.30 from 2008 to 2013 and 4.44 ± 0.33 from 2013 to 2019. There are 9 earthquakes whose magnitudes are bigger than and equal to 5.0 from 1974 to 2002 and the biggest of them is 6.3; 3 earthquakes from 2002 to 2008 and the biggest of them is 5.7; 2 earthquakes from 2008 to 2013 and the largest has a magnitude of 5.1; and 2 events from 2013 to 2019 and the biggest has a magnitude of 5.2 (the numbers of 4.0 ≤ M_d earthquakes were also given in Table 2). Time-magnitude distribution of the earthquakes shows that there is an important increase in the number of strong/large earthquakes after 1998 although there are few strong earthquakes between 1974 and 1998. Seismicity related to the clustering properties can be clearly seen and it can be related to a strong/large earthquake in

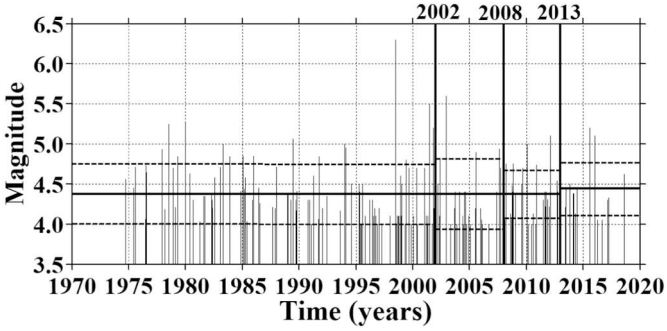

Fig. 9. Variations of earthquake magnitudes as a function of time with $M_d \geq 4.0$ including 216 earthquakes from 1970 to 2019. Original dataset was used for plotting. Thick horizontal lines indicate the mean magnitude and the upper and lower thin horizontal lines show the standard deviations for these time intervals.

Table 2
Some statistics for the earthquakes with $M_d \geq 4.0$ and $M_d \geq 5.0$ from 1970 to 2019.

Time interval	Number of earthquakes, $M_d \geq 4.0$	Average magnitude	Number of earthquakes, $M_d \geq 5.0$	Maximum magnitude
1970–2001	127	4.38 ± 0.38	9	6.3
2002–2007	45	4.38 ± 0.44	3	5.7
2008–2012	29	4.38 ± 0.30	2	5.1
2013–2018	15	4.44 ± 0.33	2	5.2

and around the CAR. In addition, clustering features of the temporal seismicity connected with 5.5 ≤ M_d earthquakes is strong enough for the most events occurred in 1998, 2001, 2002 and 2007.

GENAS test, as stated above, is an important tool for a detailed evaluation of earthquake rate changes. The aim of separately analyzing different magnitude groups is to evaluate the specific magnitude levels that individual variations observed. The results of *GENAS* application were illustrated in Fig. 10. *GENAS* results show the remarkable breaks in slope, beginning from the end of data including all magnitude levels. The statements "Mag and below" and "Mag and above" define all events with a magnitude lower than M_d and all events with a magnitude greater than M_d, respectively. As stated in many researchers such as Zúñiga et al. (2000, 2005) and Chouliaras (2009), *GENAS* modelling presumed that only independent events can be compared to refrain the false alarms from earthquake activity rate changes because of the dependent events such as aftershocks, foreshocks or earthquake clusters. Therefore, declustered dataset containing *Mcomp* (6474 events) was used in this test. *GENAS* observations show that there is a mild decrease and increase in recorded small events in 1994, and a strong decrease and increase of small earthquakes in 2005. In addition, four significant decreases of reported small earthquakes were observed between 2012 and 2014, as well as a strong decrease in small events in 2018. On the contrary, there are some weak increases of small earthquakes in 1980, 1983, 2002 and 2009. Five significant increases in small events were observed in 1995, 1996, 2003, 2008 and 2010. Some light decreases and increases of large earthquakes were reported in 1994, from 1997 to 1999, 2004 and 2018. There are three weak decreases in large earthquakes in 2012, 2014 and 2018, whereas three weak increases of large earthquakes were observed in 1996, 2003 and 2008. In addition, GENAS results indicate that two strong increases of big earthquakes were observed in 1995 and 2002, and a weak increase of large events in 2008. However, some weak and mild decreases in reported large events were observed 2010, 2012 and 2013. Thus, *GENAS* test, as stated above, provided a systematic investigation of the earthquake activity and a general overview of the earthquake history in and around the CAR.

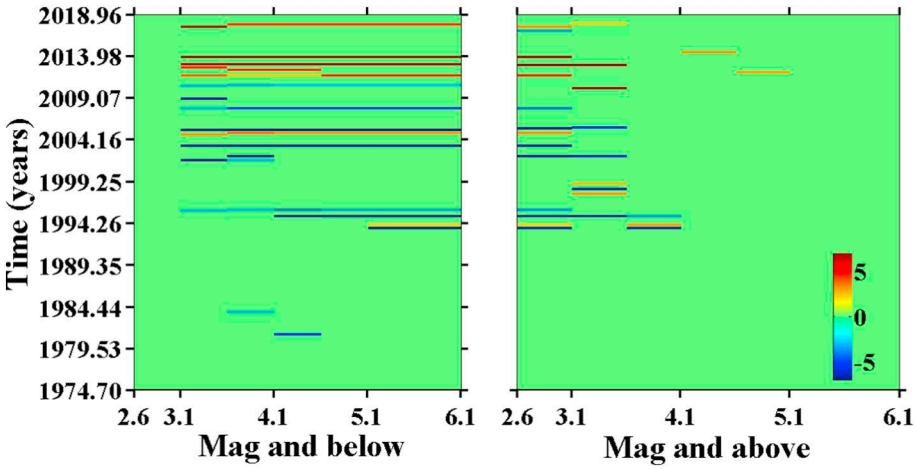

Fig. 10. The *GENAS* results for declustered dataset (6474 earthquakes). Times of the important changes were (at the 99% confidence level) indicated in blue for increasing activity rate and red for decreasing activity rate as a function of different magnitude levels. (For interpretation of the references to colour in this figure legend, the reader is referred to the web version of this article.)

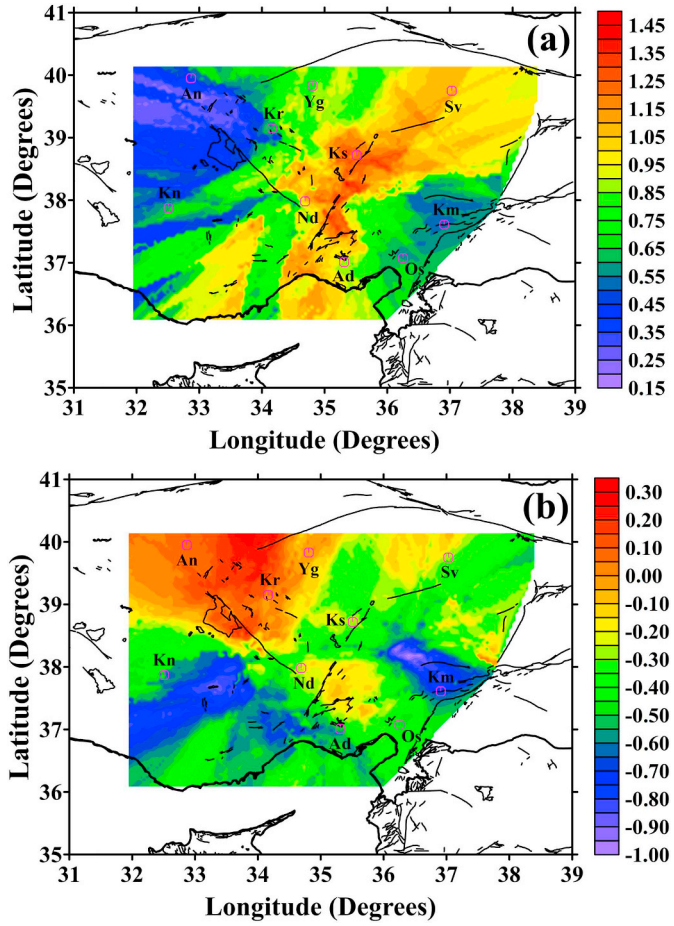

Fig. 11. Regional changes of temporal *b*-value from (a) 1974 to 2007 and (b) 2008 to 2019 in and around the CAR of Turkey. Declustered dataset was used in the analysis. Main tectonics and several provinces were also shown.

Fig. 11 shows the region-time changes of *b*-value in the CAR and its vicinity. Regional changes in *b*-value as a function of time were calculated for the time periods of 1974–2007 (Fig. 11a) and 2008–2019 (Fig. 11b). In order to image these region-time changes, declustered catalog including 15,107 earthquakes was used and study area was divided into grid cells spacing of 0.05° in latitude and longitude. As seen in Fig. 11a, there is a tendency of increase in *b*-value between 2002 and 2007 as compared to 1974–2001. On the contrary, *b*-value shows a decreasing trend in between 2013 and 2019 in comparison with 2008–2012 (Fig. 11b). At the beginning of 2019, some regions show large decreases in *b*-value changing between −0.5 and −1.0 units. These regions are located in and around the NF, KKFZ, between the MFZ and the KKFZ, in the southwestern parts of NF, in the southwestern end of the CAFZ, in SFR and its vicinity. Also, there are some small decreases (between −0.4 and −0.1 units) and increases (between 0.1 and 0.3 units) in *b*-value in the other regions at the beginning of 2019.

Seismic activity rate changes for the study region at the beginning of 2019 were given in Fig. 12. As in *b*-value map, a spatial grid of 0.05° in latitude and longitude was used in order to image *Z*-value. Time window was used as 4.5 years in order to map the temporal changes of regional distribution of Z-value. From the tests and assessments of the quiescence maps, it was concluded that quiescence regions are better imaged for a time window of 4.5 years. Compared to 1.5, 2.5, 3.5 and 5.5 years, since precursory anomalies detected in Fig. 12 are the best represented at the epicentral areas for Tw = 4.5, this time window was preferred to image the regional variations of the seismic activity rate changes. Anomaly regions exhibiting seismic quiescence at the beginning of 2019 are centered in the northwest ends of TGFZ and study

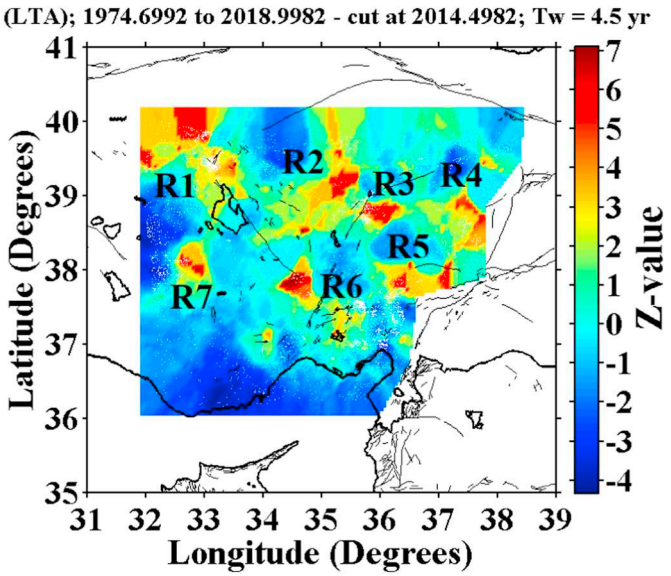

Fig. 12. Regional changes of *Z*-value at the beginning of 2019 with a time window T_W = 4.5 years in the CAR and its vicinity. White dots indicate the declustered earthquakes with $M_d \geq 2.6$ (6474 events). Major tectonics were also given. The nearest earthquakes at each node were considered as 50 and earthquake population was separated into many binning spans of 28 days to obtain a dense and continuous coverage in time.

region (R1), in northeast of SF, and between SF and the CAFZ (R2), in northeast parts of the CAFZ (R3), in the west of MLF (R4), in and around SRF (R5), in the southeast end of TGFZ between TGFZ and the CAFZ, between the CAFZ and YGFZ (R6), in the southwest of Tuzgölü (R7). These results also coincide with the findings of *GENAS* test. Thus, as shown in Figs. 11b and 12, a combination of low *b*-value and large *Z*-value regions may provide preliminary and useful keys to evaluate the earthquake potential in and around the CAR and thus, special emphasis needs to be paid to these anomaly areas.

5. Discussions

It is well known that the CAR and its vicinity has not a high-level seismic hazard with regard to strong earthquakes occurrences in the short/intermediate term. Therefore, these types of statistical assessments related to the possible correlation between seismic and tectonic parameters are quite rare. Also, there exist very few studies on the region-time characteristics of the earthquake occurrences in the CAR and its vicinity. However, a detailed statistical region-time analysis of earthquake distributions would be important since some strong earthquakes occurred in the last ten years in this region. Some researchers used different techniques to describe the statistical behaviors of earthquake occurrences in and around the CAR, and they provided important results (e.g., Dirik and Göncüoğlu, 1996; Koçyiğit, 2000; Bilim, 2003; Çobanoğlu et al., 2006; Kahraman et al., 2008; Öztürk et al., 2008; Özmen, 2015).

Dirik and Göncüoğlu (1996) made a study to describe the seismicity characteristic of the Central Anatolia and provided the general properties of neotectonic structures of the region. It is pointed out that the Central Anatolia has significant geological structures and neotectonic and paleotectonic environments are clearly evident. According to their neotectonic map, there is a general density of volcanic areas, thermal springs and most of the earthquakes along the main fault regions in the Central Anatolia. Consequently, they stated that most of the segments in this region are still tectonically active according to recent seismicity and morphotectonic behaviors.

An investigation of earthquake hazard in Çankırı, one of the largest depocenters of the Central Anatolia, was achieved by Bilim (2003) and Gumbel I distribution model was used for the statistical evaluations. For this purpose, the catalog including the earthquakes with magnitude Mb ≥ 4.0 (body wave magnitude) from 1964 to 2002 between the co-ordinated 40.30°-41.00°N latitude and 32.50°-34.50°E longitude were used. *b*-value of the Gutenberg-Richter scaling law was computed as 0.56 with the maximum likelihood method. The results show that probabilities of earthquakes with Mb ≥ 5.0 in 25, 50, 75 and 100 years were calculated as 93%, 99%, 99% and 99%, respectively. These probabilities for the earthquakes of Mb ≥ 5.5 in 25, 50, 75 and 100 years were estimated as 77%, 95%, 98% and 99%, respectively. In addition, the probabilities of Mb ≥ 6.0 earthquakes in 25, 50, 75 and 100 years were computed as 52%, 77% and 89% and 95%, respectively. However, the probabilities for Mb ≥ 6.5 earthquakes in 25, 50, 75 and 100 years were found as 22%, 39%, 52% and 63%, respectively. Also, the return periods of Mb ≥ 5.0, Mb ≥ 5.5, Mb ≥ 6.0 and Mb ≥ 6.5 earthquakes were estimated as 9, 17, 32 and 63 years, respectively (all estimated parameters can be found from Tables 3 and 4 in Bilim (2003). According to these results, a seismic hazard can be mentioned in the intermediate/long terms in the Central Anatolia.

A statistical study in order to estimate the interval of earthquake occurrences and return periods of earthquakes in the Eastern Mediterranean region, covering several parts of the CAR, was realized Çobanoğlu et al. (2006) by using different statistical approaches such as Poisson, Gumbel and Exponential distribution models. They estimated *b*-value of the Gutenberg-Richter relation as 0.96 for study area. According to their results of Poisson model including seismic risk and recurrence times, probabilities of Ms. = 5.0 (surface wave magnitude) earthquakes in 10, 20, 50, 75 and 100 years were calculated as 75%, 94%, 99%, 99%, and 100%, respectively. The probabilities of Ms = 5.5 earthquakes in 10, 20, 50, 75 and 100 years were found as 37%, 60%, 90%, 97%, and 99%, respectively. Also, the probabilities of Ms = 6.0 earthquakes in 10, 20, 50, 75 and 100 years were calculated as 14%, 26%, 53%, 68% and 78%, respectively. However, probabilities of Ms = 6.4 earthquakes in 10, 20, 50, 75 and 100 years were estimated as 6%, 12%, 27%, 38% and 47%, respectively. Also, the return periods of Ms = 5.0, 5.5, 6.0 and 6.4 earthquakes were computed as 7.3, 21.8, 65.9 and 159.6 years, respectively (all details for the other model results can be found from Table 7 in Çobanoğlu et al., 2006). As seen from the results of Bilim (2003) and Çobanoğlu et al. (2006), there is a significant earthquake potential in the intermediate/long terms in several regions of the Central Anatolia.

Kahraman et al. (2008) made a probabilistic seismic hazard assessment for the western Anatolian region of Turkey by considering the Gutenberg-Richter power law. *b*-value of magnitude-frequency relation was calculated as 0.84 with the maximum likelihood estimation for a seismic catalog from 1900 to 2005. According to their Poisson model results, probabilities of M ≥ 5.0, M ≥ 5.5 and M ≥ 6.0 earthquakes in 50, 75 and 100 years were computed as 100% for all magnitude ranges. However, the probabilities of M ≥ 6.5 earthquakes in 50, 75 and 100 years were found as 94.8%, 98.8% and 99.7%, respectively, while the probabilities of M ≥ 7.0 earthquakes in 50, 75 and 100 years were estimated as 64.7%, 81.4% and 89.4%, respectively. Also, the return periods of M ≥ 5.0, M ≥ 5.5, M ≥ 6.0, M ≥ 6.5 and M ≥ 7.0 earthquakes were calculated as 1.3, 3.5, 9.8, 27.1 and 75.1 years, respectively (all statistical results of the other models can be found from Tables 6 and 8 in Kahraman et al., 2008). Thus, seismic hazard in the western Anatolian region of Turkey was statistically analyzed considering the probability of occurrence and the return periods of certain earthquakes, and as a remarkable fact, these results coincide with the findings of Bilim (2003) and Çobanoğlu et al. (2006) in the intermediate/long terms.

Öztürk et al. (2008) made a quantitative earthquake hazard assessment for different 24 sub-regions of Turkey by using Gumbel I distribution model. They estimated several parameters such as the recurrence time, possible maximum magnitude and probabilities of great earthquakes for some magnitudes and periods. Region 22 (Mid Anatolian Fault System) in their study corresponds to the region in the present study. According to their results, *b*-value of magnitude-frequency law was estimated as 0.74 through Gumbel I method. Their results show that probabilities of earthquakes with Ms = 5.0 in 10, 25, 50 and 100 years were estimated as 67.4%, 93.9%, 99.6% and 100%, respectively. These probabilities for the earthquakes of Ms = 5.5 in 10, 25, 50 and 100 years were calculated as 38%, 69.7%, 90.8% and 99.2%, respectively. In addition, the probabilities of Ms = 6.0 earthquakes in 10, 25, 50 and 100 years were found as 18.4%, 39.9% and 63.9% and 87%, respectively. However, the probabilities for Ms = 6.5 earthquakes in 10, 25, 50 and 100 years were computed as 8.3%, 19.5%, 35.2% and 58.1%, respectively. Also, mean return periods of Ms. = 5.0, 5.5, 6.0 and 6.5 earthquakes were estimated as 8.91, 20.89, 48.98 and 114.82 years, respectively (all calculated parameters can be found from Tables 3 and 4 in Öztürk et al., 2008). According to these findings, an intermediate/long terms earthquake hazard can be mentioned in and around the CAR.

Özmen (2015) carried out a statistical earthquake hazard analysis for the Central Anatolia region of Turkey by using the earthquakes with Mw ≥ 4.0 (moment magnitude) in time interval between 1900 and 2011. For this purpose, Gumbel Extreme Values approach was used to estimate the seismic hazard parameters and the evaluation was provided by considering the past events in six sub-regions limited by the co-ordinates 30°E and 35°E in longitude and the co-ordinates 38°N and 41.0°N in latitude. Earthquake probabilities and recurrence periods for each sub-region were calculated for strong/large events that may cause damage and occur in the next. The comparison of different sub-regions indicates that the NAFZ has the highest earthquake hazard with the

probability of Mw ≥ 7.0 earthquake (87%) in the next 100 years with a return period of 50 years and therefore, the NAFZ may be a significant source for an earthquake-related hazard in the Central Anatolia region. As a remarkable fact, this evaluation of Özmen (2015) may contribute to seismic hazard studies and the results can provide preliminary and useful statistics for the assessment of earthquake potential in this region.

Based on the results in this study and the observations from literature, region-time analysis of earthquake behaviors in the CAR and its vicinity in recent years may provide preliminary and useful results for the near future earthquake hazard. Although the CAR was not struck with a great/devastating earthquake in the past and recent years, several strong/large earthquakes such as "*M*5.6-Kahramanmaraş, December 14, 2002; "*M*5.7-Anakara, December 20, 2007; *M*5.1-Kırşehir, January 10, 2016" occurred in the study region. As seen from the studies of mentioned researchers, all results coincide with each other and with this study and therefore, a region-time correlation between these seismic and tectonic parameters may supply an important perspective of hazard and risk for strong/large earthquake occurrences in the Central Anatolian region of Turkey in the intermediate/long terms.

6. Conclusions

A statistical region-time evaluation of the seismicity in and around the Central Anatolian region of Turkey was carried out by using recent earthquake catalog at the beginning of 2019. For this purpose, the most frequently used seismic and tectonic parameters such as the seismic *b*-value, seismic quiescence *Z*-value, *GENAS* application, annual probability and return period of the earthquakes were preferred to analyze.

There is a tendency to increase in the earthquake activity rate after 2002, especially after 2008 and approximately 81.65% of the events in the catalog occurred between 2008 and 2019. Magnitude completeness for all catalog was estimated as 2.6 and average *b*-value of all earthquake occurrences was calculated as 1.08 ± 0.03. This *b*-value means that earthquake occurrences in and around the CAR is well represented by the Gutenberg-Richter scaling law. A noticeable increase was observed in *b*-value (1.58 ± 0.03) from 2002 to 2008. On the contrary, there is a clear decrease in *b*-value between 2008 and 2019. *b*-value was estimated as 1.48 ± 0.03 between the years 2008 and 2012, as 1.25 ± 0.05 between the years 2013 and 2019. Therefore, this decreasing trend in *b*-value in recent years may be related to increasing stress release and accordingly the next possible earthquake in study region.

Time-magnitude analyses of annual probabilities and return periods for the specific magnitude levels of the strong/large earthquakes reveals that the CAR and surrounding regions has an intermediate or long terms seismic hazard after the year of 2021 for the probability of occurrence of strong or large earthquakes with $M_d \geq 5.0$. The *GENAS* modelling of earthquakes shows that important seismicity rate changes affecting different magnitude levels take places in different time intervals. Thus, investigation of these decreases and increases for small/large events allow to determine the most significant changes in earthquake catalog.

Regional changes in *b*-value as a function of time show remarkable fluctuations. A significant decrease was observed in spatial variations of temporal *b*-values for the time period of 2013 to 2019 in comparison with those for the time intervals of 2002 to 2007 and 2008 to 2013. These anomaly regions cover NF and its vicinity along the southern, western, southwestern and northwestern directions, the MFZ, KKFZ, KOFZ, SRF and along its northwestern part, the area between SRF and EAFZ. Seven significant anomaly regions exhibiting seismic quiescence were detected at the beginning of 2019. These regions with high *Z*-value can be given as the northwestern ends of the TGFZ and study area including AF, the northeast of SF, between SF and the CAFZ, the northeastern parts of the CAFZ, the west of MF, between SRF and the EAFZ, the southeastern end of the TGFZ, KKFZ and its vicinity, the southwest of Tuzgölü. Thus, these anomaly areas of *b*-value and *Z*-value defined in and around the CAR at the beginning of 2019 may be interpreted as the most probable regions for the future strong/large main shocks.

As a remarkable fact, decreases in the *b*-value, increases in *Z*-value, the results of return periods of earthquakes and of the *GENAS* application may be related to stress increase and they can provide the preliminary reports for the earthquake potential in the CAR. Therefore, a correlation and combined interpretation between these parameters can give useful preliminary results on local seismicity and seismic risk and, can be potentially lead to hazard studies in this region.

Declaration of competing interest

The authors declare that they have no known competing financial interests or personal relationships that could have appeared to influence the work reported in this paper.

Acknowledgements

The author would like to thank to the Editor and reviewers for their useful and constructive suggestions in improving this paper. I thank to KOERI and AFAD for providing free earthquake database via internet.

References

Aki, K., 1965. Maximum likelihood estimate of b in the formula log $N = a$-bM and its confidence limits. Bulletin of the Earthquake Research Institute, Tokyo University 43, 237–239.
Ali, S.M., 2016. Statistical analysis of seismicity in Egypt and its surroundings. Arab. J. Geosci. 9, 52.
Bilim, F., 2003. Investigation of seismic hazard in Çankırı, Turkey, using Gumbel's first asymptotic distribution of extreme values. J. Balkan Geophys. Soc. 6 (3), 158–164.
Bozkurt, E., 2001. Neotectonics of Turkey-a synthesis. Geodin. Acta 14, 3–30.
Chiba, K., 2019. Spatial and temporal distributions of b-values related to long-term slow-slip and low-frequency earthquakes in the Bungo Channel and Hyuga-nada regions, Japan. Tectonophysics 757, 1–9.
Chouliaras, G., 2009. Investigating the earthquake catalog of the National Observatory of Athens. Natural Hazards Earth System Sciences 9, 905–912.
Coban, K.H., Sayil, N., 2019. Evaluation of earthquake recurrences with different distribution models in western Anatolia. J. Seismol. 23, 1405–1422.
Çobanoğlu, İ., Bozdağ, Ş., Dinçer, İ., Erol, H., 2006. Statistical approaches to estimating the recurrence of earthquakes in the eastern Mediterranean region. İstanbul Univ. Eng. Fac. Earth Sci. J. 19 (1), 91–100 (in Turkish with English abstract).
Console, R., Montuori, C., Murru, M., 2000. Statistical assessment of seismicity patterns in Italy: are they precursors of subsequent events? J. Seismol. 4, 435–449.
Dirik, K., Göncüoğlu, M.C., 1996. Neotectonic characteristics of Central Anatolia. Int. Geol. Rev. 38, 807–817.
Frohlich, C., Davis, S., 1993. Teleseismic b-values: or, much ado about 1.0. J. Geophys. Res. 98 (B1), 631–644.
Gök, E., Polat, O., 2014. An assessment of the microseismic activity and focal mechanisms of the Izmir (Smyrna) area from a new local network. IzmirNET. Tectonophysics 635, 154–164.
Gökten, E., Varol, B., 2010. General geology of the region and seismic sources. In: Başokur, A. (Ed.), Geological-Geophysical-Geotechnical Properties of Soils West of the City of Ankara and Dynamic Behavior. Ankara University, pp. 12–32 (in Turkish).
Gutenberg, B., Richter, C.F., 1944. Frequency of earthquakes in California. B. Seismol. Soc. Am. 34, 185–188.
Habermann, R.E., 1983. Teleseismic detection in the Aleutian Island arc. J. Geophys. Res. 88 (B6), 5056–5064.
Joseph, J.D.R., Rao, K.B., Anoop, M.B., 2011. A study on clustered and de-clustered world-wide earthquake data using G-R recurrence law. International Journal of Earth Sciences and Engineering 4, 178–182.
Kahraman, S., Baran, T., Saatçı, İ.A., Şalk, M., 2008. The effect of regional borders when using the Gutenberg-Richter model, case study: western Anatolia. Pure Appl. Geophys. 165, 331–347.
Katsumata, K., 2011. Precursory seismic quiescence before the Mw = 8.3 Tokachi-oki, Japan, earthquake on 26 September 2003 revealed by a re-examined earthquake catalog. J. Geophys. Res. 116, B10307, doi:https://doi.org/10.1029/2010JB007964.
Katsumata, K., Kasahara, M., 1999. Precursory seismic quiescence before the 1994 Kurile Earthquake (Mw = 8.3) revealed by three independent seismic catalogs. Pure Appl. Geophys. 155, 43–470.
Koçyiğit, A., 2000. General neotectonic characteristics and seismicity of Central Anatolia: Haymana-Tuzgölü-Ulukışla basins applied study (workshop). Turk. Pet. Geol. Spec. Publ. 5, 1–26 (in Turkish).
Mogi, K., 1962. Magnitude-frequency relation for elastic shocks accompanying fractures of various materials and some related problems in earthquakes. Bulletin of the Earthquake Research Institute, Tokyo University 40, 831–853.

Negi, S.S., Paul, A., 2015. Space time clustering properties of seismicity in the Garhwal-Kumaun Himalaya, India. Himal. Geol. 36 (1), 91–101.
Ormeni, R., Öztürk, S., Fundo, A., Çelik, K., 2017. Spatial and temporal analysis of recent seismicity in different parts of the Vlora-Lushnja-Elbasania-Dibra Transversal Fault Zone, Albania. Austrian Journal of Earth Sciences 110 (2), doi:10.17738/ajes.2017.0015.
Ozer, C., Gok, E., Polat, O., 2018. Three-dimensional seismic velocity structure of the Aegean region of Turkey from local earthquake tomography. Ann. Geophys. 61 (1), 111–121.
Ozer, C., Ozyazicioglu, M., Gok, E., Polat, O., 2019. Imaging the crustal structure throughout the east Anatolian fault zone, Turkey, by local earthquake tomography. Pure Appl. Geophys. 176 (6), 2235–2261.
Özmen, B., 2015. Assessment of the statistical earthquake hazard parameters for the Central Anatolia region. Turkey. Arab. J. Geosci. 8, 6341–6351.
Özsayın, E., Dirik, K., 2007. Quaternary activity of the Cihanbeyli and Yeniceoba fault zones: İnönü-Eskişehir fault system. Central Anatolia. Turk. J. Earth Sci. 16, 471–492.
Öztürk, S., 2009. An Application of the Earthquake Hazard and Aftershock Probability Evaluation Methods to Turkey Earthquakes. PhD Thesis, Karadeniz Technical University, Trabzon, Turkey (in Turkish with English abstract).
Öztürk, S., 2011. Characteristics of seismic activity in the western, central and eastern parts of the north Anatolian fault zone, Turkey: temporal and spatial analysis. Acta Geophysica 59 (2), 209–238.
Öztürk, S., 2013. A statistical assessment of current seismic quiescence along the north Anatolian fault zone: earthquake precursors. Austrian J. Earth Sci. 106 (2), 4–17.
Öztürk, S., 2017. Space-time assessing of the earthquake potential in recent years in the eastern Anatolia region of Turkey. Earth Sci. Res. J. 21 (2), 67–75.
Öztürk, S., 2018. Earthquake hazard potential in the eastern Anatolian region of Turkey: seismotectonic *b* and *Dc*-values and precursory quiescence *Z*-value. Front. Earth Sci. 12 (1), 215–236.
Öztürk, S., Bayrak, Y., Çınar, H., Koravos, G.Ch., Tsapanos, T.M., 2008. A quantitative appraisal of earthquake hazard parameters computed from Gumbel I method for different regions in and around Turkey. Nat. Hazards 47, 471–495.
Polat, O., Gok, E., Yılmaz, D., 2008. Earthquake hazard of the Aegean extension region (West Turkey). Turk. J. Earth Sci. 17, 593–614.
Raub, C., Martínez-Garzón, P., Kwiatek, G., Bohnhoff, M., Dresen, G., 2017. Variations of seismic b-value at different stages of the seismic cycle along the north Anatolian fault zone in northwestern Turkey. Tectonophysics 712-713, 232–248.
Reasenberg, P.A., 1985. Second-order moment of Central California seismicity, 1969-1982. J. Geophys. Res. 90 (B7), 5479–5495.
Rehman, K., Ali, A., Ahmed, S., Ali, W., Ali, A., Khan, M.Y., 2015. Spatio-temporal variations of *b*-value in and around north Pakistan. Journal of Earth System Science 124 (7), 1445–1456.
Rodriguez-Perez, Q., Zuniga, F.R., 2018. Imaging b-value depth variations within the Cocos and Rivera plates at the Mexican subduction zone. Tectonophysics 734-735, 33–43.
Şaroğlu, F., Emre, O., Kuşcu, O., 1992. Active Fault Map of Turkey. General Directorate of Mineral Research and Exploration. Ankara, Turkey.
Scholz, C.H., 1968. The frequency-magnitude relation of microfracturing in rock and its relation to earthquakes. B. Seismol. Soc. Am. 58, 399–415.
Ulusay, R., Tuncay, E., Sönmez, H., Gökçeoğlu, C., 2004. An attenuation relationship based on Turkish strong motion data and iso-acceleration map of Turkey. Eng. Geol. 74 (3–4), 265–291.
Uner, S., Ozsayin, E., Selcuk, A.S., 2019. Seismites as an indicator for determination of earthquake recurrence interval: a case study from Erciş fault (eastern Anatolia-Turkey). Tectonophysics 766, 167–178.
Utsu, T., 1971. Aftershock and earthquake statistic (III): analyses of the distribution of earthquakes in magnitude, time and space with special consideration to clustering characteristics of earthquake occurrence (1). Journal of Faculty of Science, Hokkaido University. Series VII (Geophysics) 3, 379–441.
Wiemer, S., 2001. A software package to analyze seismicity: ZMAP. Seismol. Res. Lett. 72 (3), 373–382.
Wiemer, S., Wyss, M., 1994. Seismic quiescence before the Landers (M = 7.5) and Big Bear (M = 6.5) 1992 earthquakes. B. Seismol. Soc Am. 84 (3), 900–916.
Wiemer, S., Wyss, M., 2000. Minimum magnitude of completeness in earthquake catalogs: examples from Alaska, the Western United States, and Japan. B. Seismol. Soc. Am. 90 (3), 859–869.
Wu, Y.M., Chiao, Y.L., 2006. Seismic quiescence before the 1999 Chi-Chi, Taiwan, M_W7.6 earthquake. B. Seismol. Soc. Am. 96 (1), 321–327.
Wyss, M., 1997. Second round of evaluations of proposed earthquake precursors. Pure Appl. Geophys. 149 (1), 3–16.
Wyss, M., Habermann, R.E., 1988. Precursory seismic quiescence. Pure Appl. Geophys. 126 (2–4), 319–332.
Wyss, M., Martirosyan, A.H., 1998. Seismic quiescence before the M7, 1988, Spitak earthquake, Armenia. Geophys. J. Int. 134 (2), 329–340.
Zúñiga, R.F., Reyes, M.A., Valdés, C., 2000. A general overview of the catalog of recent seismicity compiled by the Mexican Seismological Survey. Geofis. Int. 39 (2), 161–170.
Zúñiga, R.F., Reyners, M., Villamor, P., 2005. Temporal variations of the earthquake data in the catalogue of seismicity of New Zealand. Bull. N. Z. Soc. Earthq. Eng. 38 (2), 87–105.